KFUPM
Journal of Undergraduate Research International

Diamond Open Access

Article
Material Science and Engineering

Sputtered TiO_2/Al_2O_3 Multilayer Coatings as Transparent Anti-Soiling Solutions for Solar Photovoltaics in Humid–Arid Regions

Ghadah Khalid Mobaireek and Amir Al-Ahmed*

Cite https://doi.org/10.64589/juri/221312

Submitted: December 04, 2025 **Revised:** February 02, 2026 **Accepted:** February 04, 2026

ABSTRACT

Under the backdrop of Saudi Vision 2030, the Kingdom of Saudi Arabia is expanding its solar energy sector. However, soiling and high humidity in coastal arid regions such as Dhahran considerably reduce photovoltaic (PV) module efficiency. This study was aimed at investigating the deposition and optimization of multilayer anti-soiling coatings fabricated using reactive DC magnetron sputtering to mitigate dust accumulation on solar panel surfaces. Three thin-film configurations were deposited on glass substrates: a TiO_2 monolayer, a TiO_2/Al_2O_3 bilayer, and a $TiO_2/Al_2O_3/TiO_2$ sandwich structure. The samples were annealed at temperatures ranging from 100 to 400 ° C and characterized in terms of optical transmittance, surface wettability, and field durability. The results demonstrate that the layer configuration considerably influences the coating performance. The bilayer film annealed at 200 ° C exhibits the optimal light transmission and higher water contact angle of 66°. Overall, this study presents a transparent and durable coating solution to mitigate soiling losses in humid and arid climates.

Keywords: anti-soiling, coatings, solar panels, TiO_2, hydrophobicity, sputtering

1. INTRODUCTION

In recent years, the Kingdom of Saudi Arabia (KSA) has focused on diversifying its energy sector to integrate and expand clean energy sources. Under the backdrop of Saudi Vision 2030, the country aims to reduce the long-term dependence on hydrocarbons and increase investment in sustainable energy [1]. Saudi Arabia receives among the highest solar irradiance worldwide (approximately 5,644 Wh/m^2 per day) and experiences long average sunlight durations (approximately 8.9 h per day) [2]. Under these conditions, photovoltaic (PV) solar energy represents one of the most effective technologies for electricity generation. Notably, Saudi Vision 2030 seeks to increase renewable energy production to 60 GW, with 66.67% generated from solar and the remainder from wind [3]. Moreover, the national target is to produce half of all electricity from renewable energy sources by 2030 [4]. In this context, PV technology is favored owing to its cost-effectiveness, scalability, and robustness. The cost of rooftop PV systems has decreased considerably, by nearly 80%, to approximately 3.75 SAR per watt [5]. Additionally, this technology is highly scalable, with a rooftop PV system covering an industrial building of approximately 29,000 m^2 in Abqaiq City, Saudi Arabia, and demonstrating high performance ratios (approaching 94.2%) [6].

Despite these advantages, PV deployment in Saudi Arabia faces major environmental challenges. Soiling is a primary problem arising from the arid climate, where dust and sand particles accumulate on solar panels, blocking sunlight and ultimately reducing energy efficiency. A study conducted in Dhahran, Saudi Arabia, indicates that PV modules left uncleaned for six months can lead to a 50% reduction in power output [7]. Another notable problem is high humidity, especially in coastal regions such as Dhahran. Humidity levels can reach as high as 73% [8], resulting in increased light scattering and reflection, which can degrade PV performance [9]. Studies have reported a 40% power drop at 76.32% humidity, with efficiency decreasing from 12.04% to 9.7% as humidity rises from 48% to 60% [10]. Additionally, humidity promotes the adhesion of dust to PV systems via the formation of mud layers through capillary forces between condensed vapor and dust particles; these deposits are challenging to remove. Humidity also increases particulate adhesion, creating a localized environment that can promote long-term corrosion and delamination within PV modules [11]. Considering these aspects, effective cleaning strategies for PV solar panels are crucial to ensure performance in arid regions. Existing cleaning approaches can be classified into natural, mechanical/electromechanical, electrostatic, and surface-coating-based methods. Natural cleaning relies on rainfall and wind. Although water washing represents an effective cleaning method, this resource is limited in arid areas [12]. Mechanical methods such as robotic wipers and vibration systems are effective and can restore up to 99.9% of the original performance. Nevertheless, they are cost-intensive and require continuous maintenance [13]. Electrostatic methods, including electrodynamic screens, use electric fields to repel dust with over 90% efficiency. Although this solution is water-free and suitable for arid regions, it requires an external power source [14].

Among coatings, hydrophobic layers can repel water and promote particle removal; hydrophilic coatings facilitate wetting and dirt repellence; and anti-static coatings reduce dust adhesion. In arid regions, coatings are particularly promising because they maintain non-wetting properties under humid conditions, preventing dust adhesion. Moreover, coatings enable self-cleaning with minimal moisture, addressing the challenge of water scarcity.

To synthesize these coatings, TiO_2 is widely used owing to its unique properties and multifunctional photocatalytic activity. However, to improve the conductivity of TiO_2 for photovoltaic applications [15], it remains crucial to enhance the separation and mobility of electron–hole pairs while reducing their recombination to extend carrier lifetime.

Overall, an ideal anti-soiling coating for conditions prevalent in the KSA must meet several requirements: First, it should exhibit high optical transparency to maximize solar transmission to PV cells. Second, it must be mechanically strong and durable to survive the harsh environmental conditions, such as high temperatures, intense ultraviolet (UV) radiation, and sandstorms. Lastly, the coating must be scalable and easy to apply over large areas. Among thin-film synthesis techniques, physical vapor deposition (PVD), specifically, magnetron sputtering, is a promising approach [16]. Sputtering offers precise control over film thickness, composition, and adhesion, which are critical for tuning optical, mechanical, and anti-soiling performance.

Considering these aspects, this study aimed to fabricate a novel anti-soiling coating via reactive DC sputtering. A $TiO_2/Al_2O_3/TiO_2$ multilayer structure was selected because TiO_2 provides excellent self-cleaning properties, while Al_2O_3 acts as a barrier, thereby reducing charge recombination and improving durability [17]. The sputtering process was optimized to achieve a balance among transparency, durability, and dust-repellent properties for deployment in humid and arid regions.

2. METHODOLOGY

2.1. Substrate Preparation. Glass substrates were cleaned via ultrasonication (Branson 3510 Ultrasonic Cleaner, USA) for 10 min in each of the following solutions: Hellmanex cleaning solution, deionized water, acetone, and isopropyl alcohol. Before deposition, the samples were placed in a UV–ozone cleaner (Ossila, K) to remove contaminants and improve surface wettability. Half of the selected samples were covered to create reference areas for comparison between coated and uncoated surfaces.

2.2. Thin-Film Deposition. Coatings were deposited using an NCS-3000 magnetron sputtering system (NANO-MASTER, Inc., USA). The structure consisted of TiO_2 and Al_2O_3 arranged in a $TiO_2/Al_2O_3/TiO_2$ sequence. High-purity ceramic targets were used. Samples were rotated during deposition and placed 16 cm from the target. The base pressure was 4.38×10^{-5} Torr, and the working pressure was maintained at 7.95×10^{-3} Torr using argon gas. Radio frequency power of 100 W was found to be excessive, whereas 10 W led to insufficient film formation. Therefore, a power of 50 W was selected for all deposition steps. Argon flow rates were 55 sccm for TiO_2 and 12 sccm for Al_2O_3. All depositions were performed at 25-30 ° C temperature for a total duration of 1 h. After deposition, the samples were annealed at 100, 200, 300, and 400 ° C to evaluate the effect of temperature on film properties. Annealing was performed in ambient air, and the samples were then allowed to cool to room temperature.

2.3. Characterization. The optical transmittance and absorbance of the coated glass were determined using a V-670 JASCO UV-Vis/near-infrared (NIR) spectrophotometer (Japan). Surface wettability was measured using a KRÜSS DSA25 drop-shape analyzer (Germany) to determine hydrophobic or hydrophilic behavior. Field testing was performed by

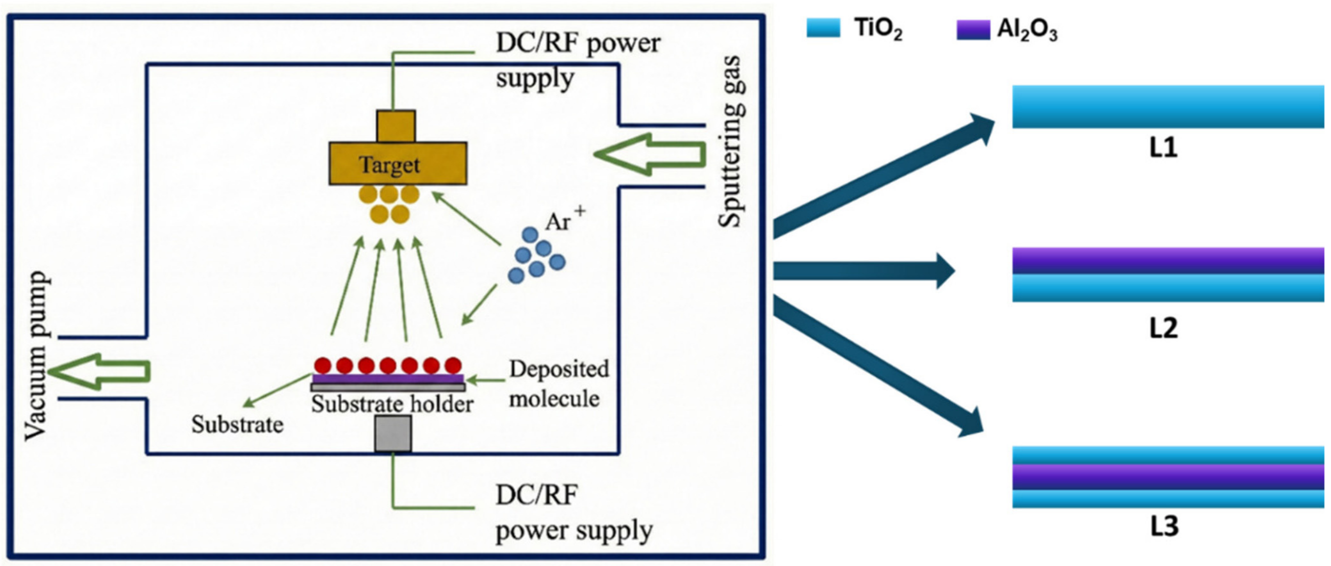

Figure 1. Schematic illustration of the magnetron sputtering deposition setup used for the fabrication of anti-soiling coatings on glass substrates. The diagram shows the sputtering target, plasma generation, and substrate positioning during deposition. This process enables the formation of uniform thin films that modify the surface properties of the glass, improving resistance to dust adhesion and enhancing anti-soiling performance

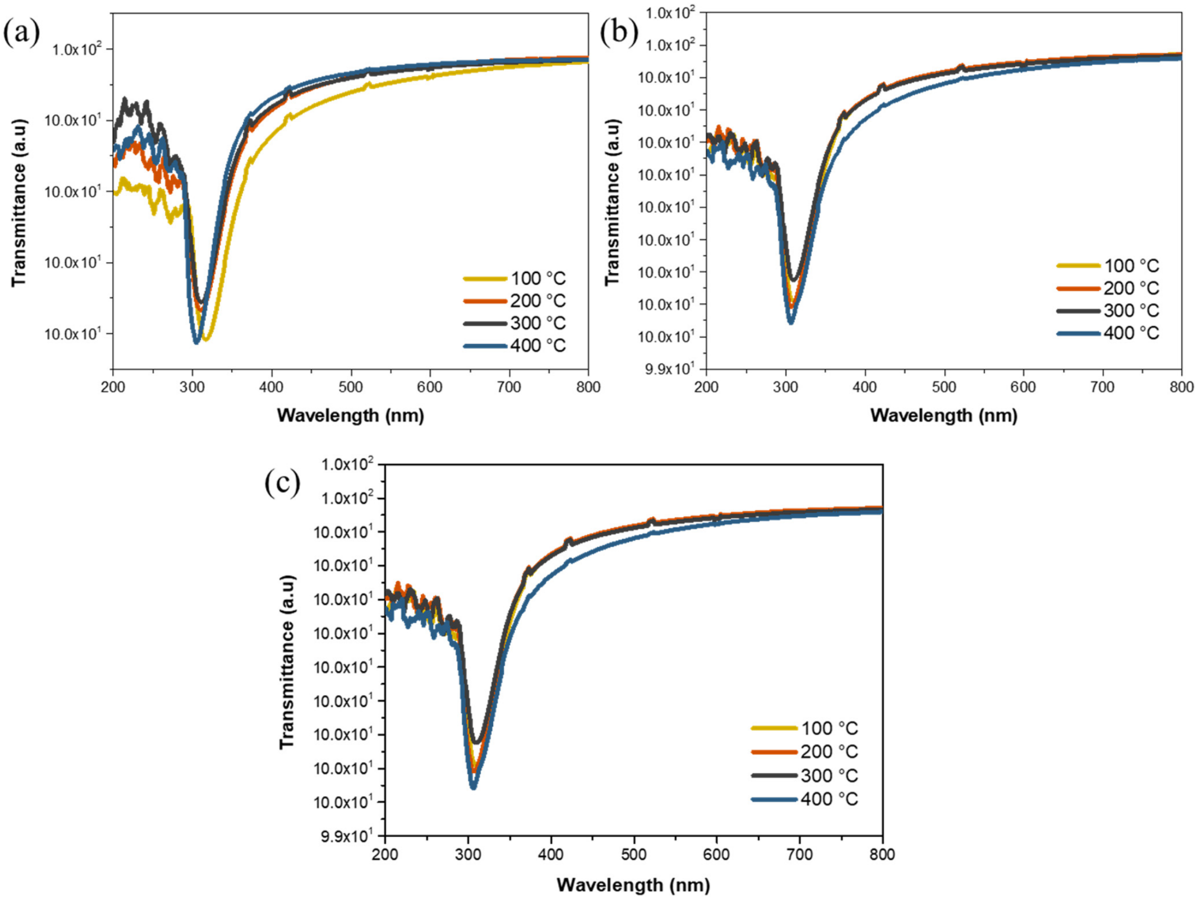

Figure 2. Optical transmittance spectra of (a) TiO_2 layer (L1), (b) TiO_2/Al_2O_3 bilayer (L2), and (c) $TiO_2/Al_2O_3/TiO_2$ layer (L3) thin films annealed at different temperatures, showing high transparency in the visible region with annealing-dependent variations in optical transmittance

exposing samples to outdoor conditions for 10 days. Three samples annealed at 200 ° C were half-covered to enable a direct comparison between the coated and uncoated sides after dirt exposure. The samples were imaged using an Olympus DSX1000 digital microscope (Japan).

3. RESULTS AND DISCUSSION

Magnetron sputtering enabled uniform thin-film deposition for the anti-soiling coating (Fig. 1). A TiO_2 monolayer (L1) served as the control film. This structure was then modified by introducing Al_2O_3 in two configurations: a TiO_2/Al_2O_3 bilayer (L2) and a $TiO_2/Al_2O_3/TiO_2$ sandwich structure (L3). The deposited thin films were annealed at different temperatures for phase development and further characterization.

3.1. Optical Properties. Optical transparency represents a critical performance parameter for anti-soiling coatings on PV modules. PV operation is based on the conversion of incident photons into electron-hole pairs within the semiconductor. Therefore, a reduction in surface transparency decreases the photon flux reaching the active solar cell and device efficiency[18]. High transmittance in the visible and NIR spectrum (350-800 nm) and high absorbance in the UV region (~300 nm) are desirable. The transmission of 350–800 nm spectra enables the light to reach the PV module beneath it, thereby generating power output efficiently. The high-energy UV radiation, which is unsuitable for PV devices, is absorbed by the anti-soiling layer, preventing it from reaching the PV module. This reduces the device's overheating and can enhances its durability[18,19]. To evaluate transparency, the annealed samples were subjected to UV-Vis absorption spectroscopy (Fig. 2). For L1, annealing at 400 ° C resulted in the highest transmittance across the visible region. The sample annealed at the lowest temperature (100 ° C) resulted in the highest absorption in the UV region. Samples annealed at 200 and 300 ° C showed intermediate transmittance and UV absorption. For L2, visible transmittance decreased after annealing at 400 ° C, while samples annealed between 100 and 300 ° C maintained higher transmittance across the visible spectrum. Samples annealed at 400 and 100 ° C exhibited similar UV absorption. Given its better visible transmittance, the sample annealed at 100 ° C was deemed superior to the 400 ° C sample. The enhanced optical parameters at lower temperatures are attributable to the bilayer configuration. The L3 sandwich structure displayed similar trends. Lower annealing temperatures led to enhanced transmittance in the visible range and UV absorbance comparable to that of the 400 ° C annealed film. The results indicate that the incorporation of the Al_2O_3 layer likely led to enhanced performance at lower annealing temperatures.

3.2. Surface Wettability.

Surface wettability determines the interaction between water droplets and the coating surface and is typically evaluated through contact angle measurements. In arid environments such as Saudi Arabia, controlling wettability is essential to minimize the capillary forces induced during humid periods, which encourage dust adhesion onto the panel surface [17]. The contact angle depends on the surface energy and roughness, which are influenced by the annealing temperature 18. As shown in Fig. 3, for L1, samples annealed at 100, 200, and 400 ° C showed contact angles of 41.6°, 38.4°, and 23.6°, respectively, indicating reduced hydrophobicity with increasing temperature. For L2, the contact angles were 62.3°, 65.8°, and 59.8° for 100, 200, and 400 ° C annealing, respectively, indicating stable contact values even at higher annealing temperatures. For L3, values of 50.6°, 46.5°, and 41.4° were noted for 100, 200, and 400 ° C annealing. While this sample also showed a gradual reduction in hydrophobicity with increasing temperature, it was less notable compared with that for L1. Overall, the annealing temperature of the sputter-coated film influences both optical properties and wettability. Increasing the annealing temperature leads to reduced hydrophobic behavior.

3.3. Performance Comparison.

A comparative assessment of L1, L2, and L3 revealed that the annealing temperature plays a crucial role in the optical and surface properties. Based on visible-light transmittance, UV absorption, and surface wettability, the optimal annealing temperature was 200 ° C for L1, L2, and L3. Although L1 annealed at 400 ° C exhibited the highest visible light transmittance, the contact angle was extremely low. By contrast, L1 annealed at 200 ° C demonstrated comparable visible transmittance and UV absorption values along with a higher contact angle of 40.4°, indicating reduced hydrophilicity compared with the sample annealed at 400 ° C. Similarly, for L2 and L3, the most favorable combination of visible transmittance and UV absorption was observed for films annealed at 200 ° C. Figure 4 (a) compares the transmittance spectra of control L1 with the best-performing L2 and L3 layers. L3 demonstrated higher transmittance in the NIR region but reduced transmittance in part of the visible region, whereas L1 and L2 recorded similar but slightly lower transmittance in the visible region. Notably, L2 displayed more pronounced UV absorption than L1 and L3. Figure 4 (b) compares the contact angle values for the best-performing samples of L1, L2, and L3. The water contact angle increased from 42° for L1 to 66° and 46° for L2 and L3, respectively. Although all surfaces remained within the weakly hydrophilic range (contact angle <90°), moderate hydrophilicity is beneficial for anti-soiling in arid regions because it prevents strong chemical bonding between dust particles and the surface. This makes it easier for wind or rain to remove dust compared with highly hydrophilic surfaces, which may promote mud-layer formation in a humid atmosphere. The increased contact angle (66°) for L2 relative to L1 (pure TiO_2) is consistent with the surface-passivation effects of Al_2O_3, [17] which reduces surface energy and promotes self-cleaning, while preserving the photocatalytic activity. In summary, the L2 layer, with a thin Al_2O_3 layer on TiO_2, demonstrates the most balanced combination of visible-light transmittance, UV absorption, and wettability, indicating its superior performance as an anti-soiling coating for high-efficiency and durable PV applications.

3.4. Field Performance Test.

While laboratory characterization clarifies intrinsic properties of the coatings, the actual anti-soiling performance must be tested under real-world environments. A 10-day field test was conducted by exposing half-coated samples to outdoor conditions. After exposure, the samples were washed with water without using any brush. As shown in Fig. 5, the uncoated portion exhibited notable accumulation of fine dust particulates, whereas the coated regions appeared visibly cleaner. This indicates that the Al_2O_3 layer mitigated the electrostatic attraction of surface charge.

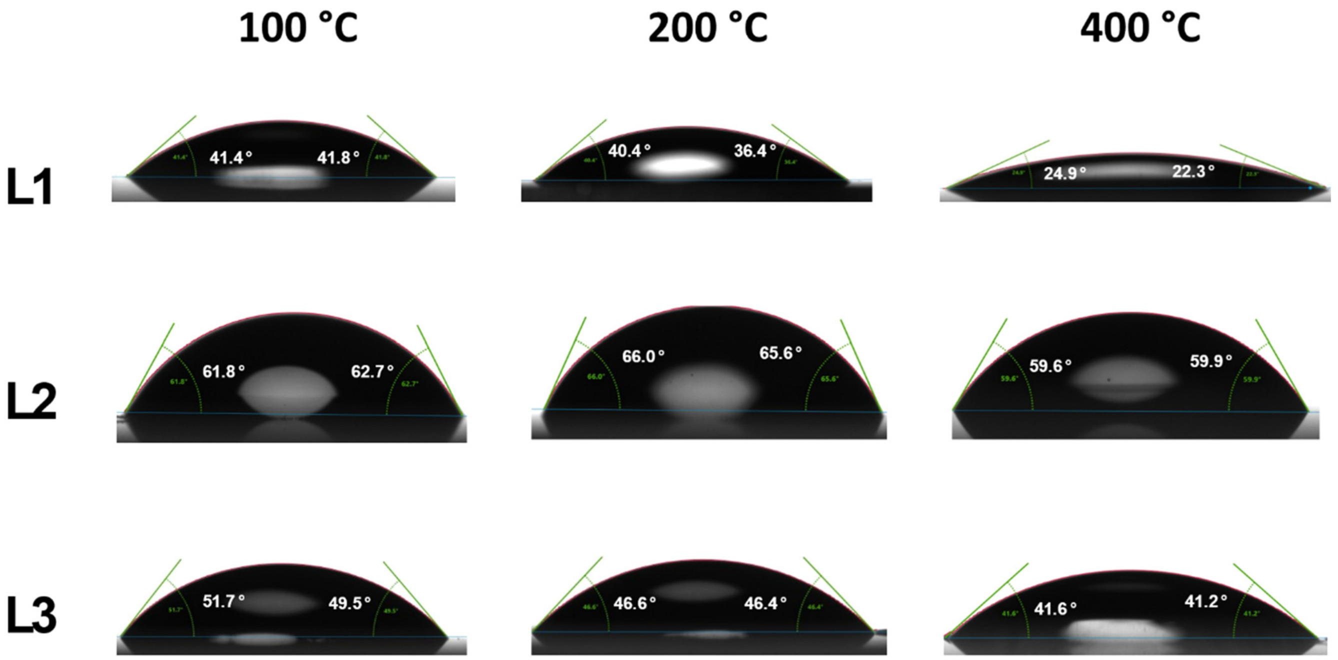

Figure 3. Contact angle measurements for L1, L2, and L3 annealed at 100, 200, and 400 ° C

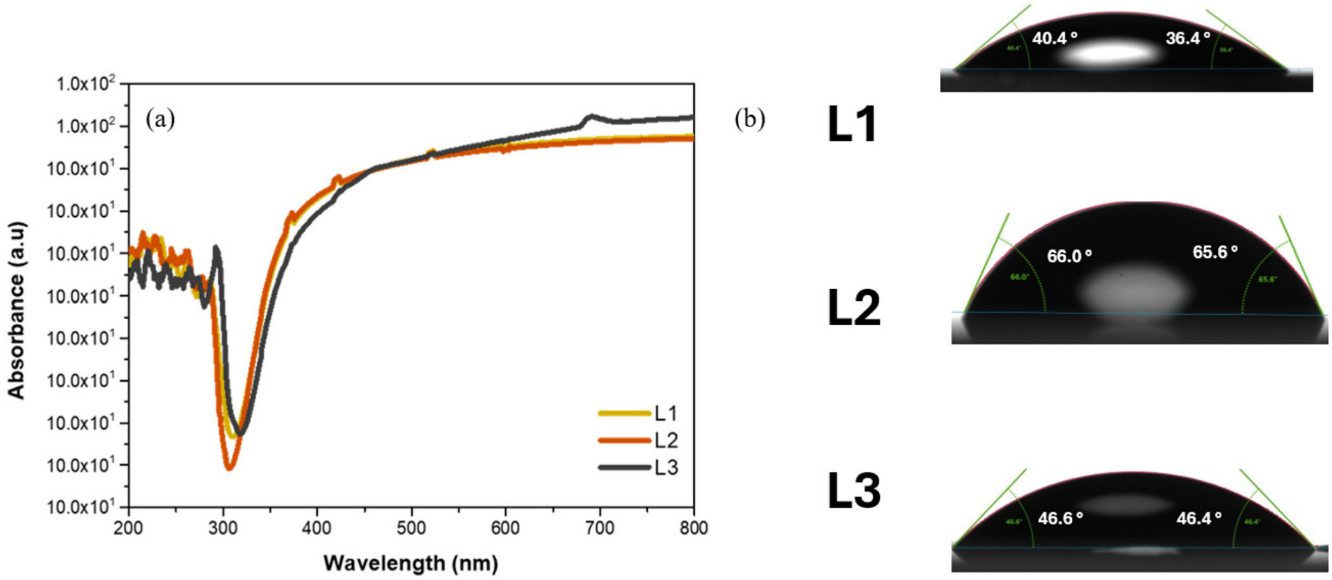

Figure 4. Water contact angle measurements for L1, L2, and L3 thin films annealed at 200 ° C

3.5. Discussion and Limitations. The findings highlight that TiO_2/Al_2O_3 multilayer coatings can mitigate performance degradation in PV modules operating under humid–arid conditions. The bilayer annealed at 200 ° C demonstrated the optimal balance of transparency and durability. However, several limitations remain to be addressed: First, while the reactive DC magnetron sputtering method provides precise control over thin film parameters, testing in this study was conducted on small-scale glass substrates. Future research can evaluate the uniformity and cost-effectiveness of this coating for large-scale PV modules. Additionally, field durability was assessed over a short period; long-term studies are necessary to determine how these multilayers behave over time. Lastly, while the 50 W power and 100–400 ° C annealing range enabled clear optimization, a broader range of deposition powers and temperatures can be explored in future work.

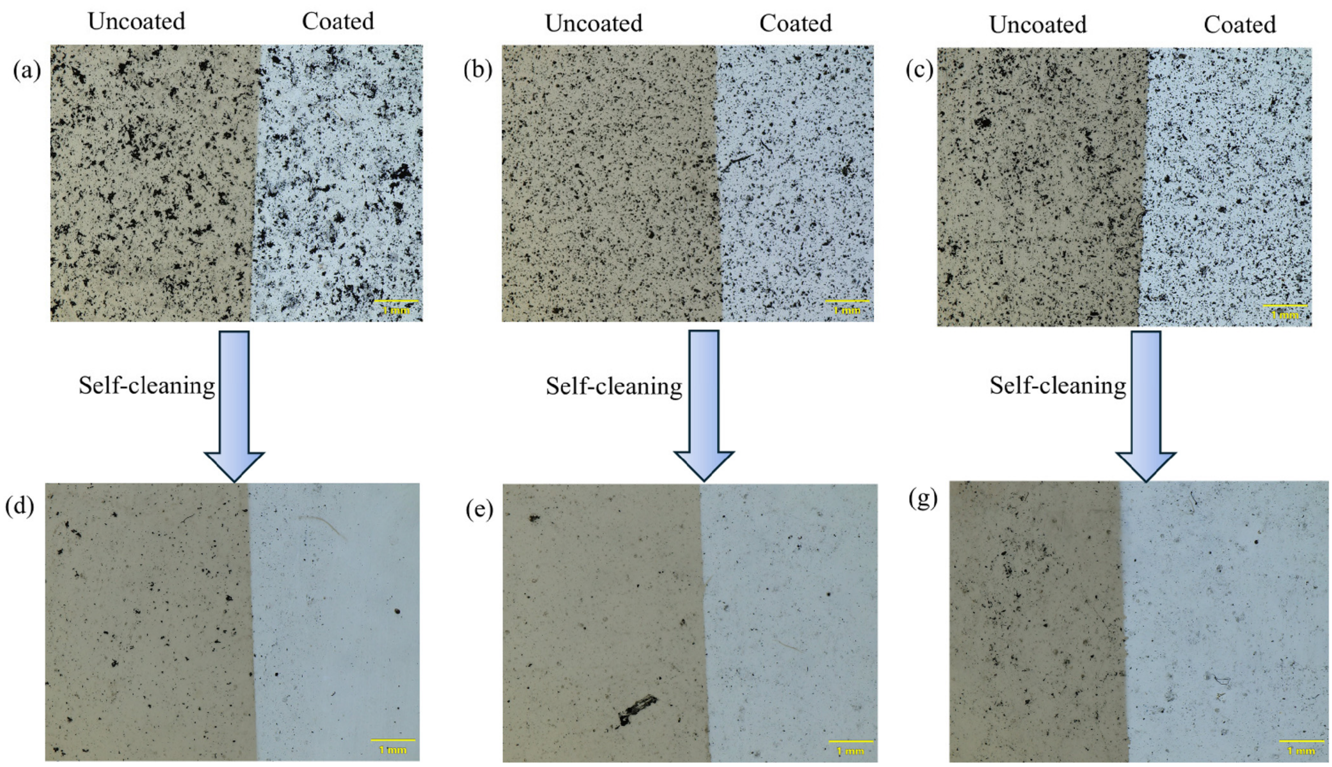

Figure 5. Optical microscopy images of (a,d) L1, (b,e) L2, and (c,g) L3 samples annealed at 200 ° C. (a–c) dust deposition before rinsing and (d, e, g) surfaces after self-cleaning. Each image compares the uncoated region (left) with the coated region (right)

4. CONCLUSION

This study addressed key environmental challenges affecting PV modules in Saudi Arabia, i.e., dust accumulation and humidity, by developing multilayer anti-soiling coatings using magnetron sputtering. The control TiO_2 coating was modified through the addition of an Al_2O_3 passivation layer and a $TiO_2/Al_2O_3/TiO_2$ sandwich structure. Among the three film configurations, L2 and L3 outperformed the control TiO_2 layer in terms of enhanced visible-light transmittance, UV absorption, and water contact angle. The L2 configuration also exhibited high transparency and could mitigate dust adhesion in field tests. Consequently, the proposed coating strategy offers an efficient solution for increasing the output of solar panels, supporting the KSA's goal to achieve 50% renewable-energy generation by 2030.

AFFILIATIONS AND AUTHOR DETAILS

Undergraduate Author

Ghadah Khalid Mobaireek – *Department of Materials Science and Engineering, King Fahd University of Petroleum & Minerals, Dhahran 31261, Saudi Arabia*; 0009-0001-5529-3045
Email: s202248500@kfupm.edu.sa

Corresponding Author

Amir Al-Ahmed – *Research Mentor, Interdisciplinary Research Center for Sustainable Energy Systems, King Fahd University of Petroleum & Minerals, Dhahran, 31261, Saudi Arabia; Lead Research Scientist, Chemistry Department, King Fahd University of Petroleum and Minerals, Dhahran, 31261, Saudi Arabia*; 0000-0001-9686-2374
Email: aalahmed@kfupm.edu.sa

ACKNOWLEDGMENTS

The authors would like to acknowledge the support provided by the Department of Materials Science and Engineering and the Interdisciplinary Research Center at King Fahd University of Petroleum and Minerals. This work was supported by the Renewable Energy Technical Incubator (RETI), Project No. CREP2522, funded by the National Industrial Development and Logistics Program (NIDLP) under the Interdisciplinary Research Center for Sustainable Energy Systems (IRC-SES), KFUPM.

REFERENCES

(1) Arif, M. S. B. & Ali, A. Transforming Saudi Arabia's energy landscape towards a sustainable future: Progress of solar photovoltaic energy deployment. *Sustainability* 15, 8420 (2023). https://doi.org/10.3390/su15108420

(2) Rehman, S., Bader, M. A. & Al-Moallem, S. A. Cost of solar energy generated using PV panels. *Renew. Sustain. Energy Rev.* 11, 1843–1857 (2007). https://doi.org/10.1016/j.rser.2006.03.005

(3) Al Zohbi, G. & AlAmri, F. G. Current situation of renewable energy in Saudi Arabia: Opportunities and challenges. *J. Sustain. Dev.* 13, 1–13 (2020). https://doi.org/10.5539/jsd.v13n2p98

(4) Saudi Green Initiative. Reducing carbon emissions. *Saudi Green Initiative* (2025). https://www.sgi.gov.sa/about-sgi/sgi-targets/reduce-carbon-emissions/

(5) M. Bolinger, R. Wiser, & E. O'Shaughnessy. Levelized cost-based learning analysis of utility-scale wind and solar in the United States. *iScience*, 25, 6, 104378, (2022) https://doi.org/10.1016/j.isci.2022.104378

(6) Al-Hanoot, A. K., Mokhlis, H., Mekhilef, S., Alghoul, M., Shareef, H. & Alotaibi, Z. Techno-economic analysis of cutting-edge PV systems deployment and reconfigurations on rooftop industrial buildings in Saudi Arabia's eastern region. *Energy Convers. Manag.: X* 25, 100873 (2025). https://doi.org/10.1016/j.ecmx.2025.100873

(7) Adinoyi, M. J. & Said, S. A. M. Effect of dust accumulation on the power outputs of solar photovoltaic modules. *Renew. Energy* 60, 633–636 (2013). https://doi.org/10.1016/j.renene.2013.06.014

(8) Climate-Top. Relative humidity in Dhahran, Saudi Arabia. *Climate-Top* (2025). https://www.climate.top/saudi-arabia/dhahran/humidity/

(9) Said, S. A. M., Hassan, G., Walwil, H. M. & Al-Aqeeli, N. The effect of environmental factors and dust accumulation on photovoltaic modules and dust-accumulation mitigation strategies. *Renew. Sustain. Energy Rev.* 82, 743–760 (2018). https://doi.org/10.1016/j.rser.2017.09.042

(10) Katkar, A. A., Shinde, N. & Patil, P. Performance and evaluation of industrial solar cell with respect to temperature and humidity. *Proc. Int. Conf. Energy, Automation and Signal*, 1–4 (2011). https://www.idc-online.com/technical_references/pdfs/mechanical_engineering/Performance{%}20and{%}20Evaluation.pdf

(11) Corn, M. The adhesion of solid particles to solid surfaces: A review. *J. Air Pollut. Control Assoc.* 11, 523–528 (1961). https://doi.org/10.1080/00022470.1961.10468032

(12) Hee, J. Y., Kumar, L. V., Danner, A. J., Yang, H. & Bhatia, C. S. The effect of dust on transmission and self-cleaning property of solar panels. *Energy Procedia* 15, 421–427 (2012). https://doi.org/10.1016/j.egypro.2012.02.051

(13) Ghodki, M. K. An infrared-based dust mitigation system operated by a robotic arm for performance improvement of solar panels. *Sol. Energy* 244, 343–361 (2022). https://doi.org/10.1016/j.solener.2022.08.064

(14) Calle, C. I., Buhler, C. R., McFall, J. L. & Snyder, S. J. Particle removal by electrostatic and dielectrophoretic forces for dust control during lunar exploration missions. *J. Electrostat.* 67, 89–92 (2009). https://doi.org/10.1016/j.elstat.2009.02.012

(15) Yao, K. J. A. et al. Sol–gel deposition of TiO2 thin films by spin coating for photovoltaic applications: Effect of acetylacetone stabilizer on structural and optical properties. *Mater. Today Proc.* (2024). https://doi.org/10.1016/j.matpr.2024.02.003

(16) Saha, R., Neha, Thukral, A., Pal, A. & Saini, P. Sunlight-responsive superhydrophilic rGO–TiO2 nanocomposite coatings for photovoltaic applications. *Diam. Relat. Mater.* 149, 111603 (2024). https://doi.org/10.1016/j.diamond.2024.111603

(17) Kim, W., Tachikawa, T., Majima, T. & Choi, W. Photocatalysis of dye-sensitized TiO2 nanoparticles with thin overcoat of Al2O3: Enhanced activity for H2 production and dechlorination of CCl4. *J. Phys. Chem. C* 113, 10603–10609 (2009). https://doi.org/10.1021/jp9008114

(18) Yang, H. & Wang, H. Numerical simulation of dust particle deposition on solar photovoltaic panels and its effect on power generation efficiency. *Renew. Energy* 201, 1111–1126 (2022). https://doi.org/10.1016/j.renene.2022.11.043

(19) Zhang, G. et al. Design and preparation of anti-reflection nanoarray structures on the surface of space solar cell glass cover. *Coatings* 13, 1092 (2023). https://doi.org/10.3390/coatings13061092

(20) Méndez-López, A. et al. Influence of annealing temperature on the structural and optical properties of ZrO2 thin films and its effect on hydrophilicity. *Crystals* 10, 454 (2020). https://doi.org/10.3390/cryst10060454